Bond graph model-based fault detection using residual sinks

W Borutzky
Bonn-Rhein Sieg University of Applied Sciences, Sankt Augustin D-53754, Germany. email: borutzky@uni-koeln.de

The manuscript was received on 8 August 2008 and was accepted after revision for publication on 23 October 2008.

DOI: 10.1243/09596518JSCE666

Abstract: In this paper, residual sinks are used in bond graph model-based quantitative fault detection for the coupling of a model of a faultless process engineering system to a bond graph model of the faulty system. By this way, integral causality can be used as the preferred computational causality in both models. There is no need for numerical differentiation. Furthermore, unknown variables do not need to be eliminated from power continuity equations in order to obtain analytical redundancy relations (ARRs) in symbolic form. Residuals indicating faults are computed *numerically* as components of a descriptor vector of a differential algebraic equation system derived from the coupled bond graphs. The presented bond graph approach especially aims at models with non-linearities that make it cumbersome or even impossible to derive ARRs from model equations by elimination of unknown variables. For illustration, the approach is applied to a non-controlled as well as to a controlled hydraulic two-tank system. Finally, it is shown that not only the numerical computation of residuals but also the simultaneous numerical computation of their sensitivities with respect to a parameter can be supported by bond graph modelling.

Keywords: bond graph modelling, quantitative model-based fault detection, fault indicators, numerical computation of residuals, residual bond graph sinks, differential algebraic equation systems, simulation of fault scenarios, parameter sensitivity of residuals

1 INTRODUCTION

As to safety, automated fault detection and isolation (FDI) and system reconfiguration are crucial in supervision and fault-tolerant closed-loop control of all kinds of industrial process engineering systems. To that end, it is obvious to compare the measured behaviour of a real system subject to faults with that of the faultless system and to use significant deviations as indicators to possible faults in some system components. The accurate behaviour can be provided by a system model. This is usually referred to as model-based fault detection. A survey of the state of the art in model-based fault detection and diagnosis can be found in reference [**1**].

The bond graph methodology [**2**–**7**] is particularly suited for modelling and for structural analysis of multidisciplinary process engineering systems [**8**–**11**]. Moreover, the use of bond graphs for *qualitative* as well as *quantitative* model-based FDI has been the subject of various recent research activities and publications [**12**–**19**]. An excellent presentation of model-based FDI using bond graphs can be found in chapter 15 of the textbook of Mukherjee *et al.* [**7**]. Other presentations of model-based FDI techniques not using bond graphs can be found, for instance, in [**20**–**22**], just to mention some textbooks out of the vast literature on FDI, fault diagnosis, and fault-tolerant control.

In model-based FDI, derivation and evaluation of so-called analytical redundancy relations (ARRs) [**23**, **24**] play a key role. They establish constraints between known variables – input variables and measured output variables – and, in general, also include known model parameters. When a process operates under normal mode conditions, evaluation of these constraints should reveal values within certain small error bounds. Theoretically, these values, also called *residuals*, should be zero. In practice, they will never be identical to zero over some time span owing to numerical inaccuracies,

sensor noise, or process parameter uncertainties. Numerical values exceeding given thresholds can serve as indicators to faults in some system components. Structural analysis of analytical constraint relations reveals whether or not faults can be isolated.

On the other hand, Borutzky and Cellier [**25**] and Borutzky [**26**] proposed to add so-called *residual sinks* to bond graphs of engineering systems in order to help identify variables for tearing the algebraic part of a differential algebraic equation (DAE) system derived from the bond graph. If the algebraic part is linear with respect to the tearing variables, mathematical software can solve it symbolically and transform the DAE system into a state space model prior to a simulation run.

In this paper, it is shown how these residual bond graph sinks can be used for the *numerical* computation of fault indicators without having to derive ARRs from model equations in symbolic form. Unlike their use in the context of tearing, in fault detection, the purpose of residual bond graph sinks is not to help reformulate the underlying DAE system. The mathematical model rather remains a DAE system.

The paper is organized as follows. The next section recalls relevant features of model-based FDI. Section 3 reconsiders residual bond graph sinks and section 4 presents the proposed bond graph approach to a numerical computation of fault indicators. In section 5, for illustration, the approach is applied to a hydraulic two-tank system as an example of a simple process engineering system. For the study of some fault scenarios, the underlying DAE system has been solved numerically by means of the open-source mathematical software package Scilab [**27**]. Section 6.2 shows that not only the numerical computation of residuals but also the simultaneous numerical computation of their sensitivities with respect to a parameter also can be supported by bond graph modelling. The paper concludes by summarizing the features of the proposed bond graph approach.

2 BOND GRAPH MODEL-BASED QUANTITATIVE FAULT DETECTION

FDI starts from a model with unknown variables. After their elimination, constraints between known variables (input variables and measured output variables) remain, defining what is called ARRs. In general, these constraints also include known model parameters. Their numerical evaluation at each time instant, t, produces a residual *res*. Under normal mode of operation it should be zero, theoretically. In practice, it always takes non-zero values owing to numerical errors, sensor noise, or parameter uncertainties. In bond graphs, such constraints arise from junctions. Each junction contributes a continuity equation for flows or efforts respectively. By using the constitutive equations of bond graph elements and by elimination of unknown variables, ARRs may be obtained in symbolic form *if* non-linearities permit necessary eliminations. The form of the set of ARRs is not unique and depends on the choice of computational causalities in a bond graph and the procedure that is applied. Moreover, algebraic dependencies indicated by causal paths in the bond graph and non-linear constitutive relations may *prevent* the elimination of unknown variables. Given that unknown variables can be eliminated, then structural analysis of each equation leads to a so-called signature in terms of known variables and system component parameters for each residual.

For illustration, consider the simple, oft-used example of a hydraulic two-tank system depicted in Fig. 1. It could be part of a closed-loop control system that ensures a certain fluid flow Q_o. Figure 2 shows a causal bond graph of the system in Fig. 1.

2.1 Structural observability and sensor placement

It is evident that for FDI, a system under study should be structurally observable. Moreover, it must be structurally controllable to enable fault-tolerant control (FTC) (necessary conditions).

In Fig. 2, the two bond graph elements of type De indicate effort sensors. They read the pressures in the tanks. Evidently, there is a causal path from each C element to a sensor. Moreover, both C storage elements could take preferred differential causality if the causality of the sensors is inverted. This means that the system with the two pressure sensors is *structurally* state observable [**28**]. The tank pressures are states that can be observed.

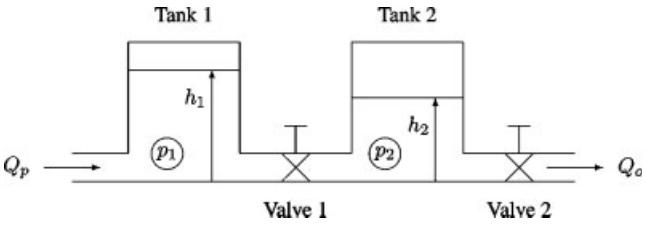

Fig. 1 Schematic of the hydraulic two-tank system

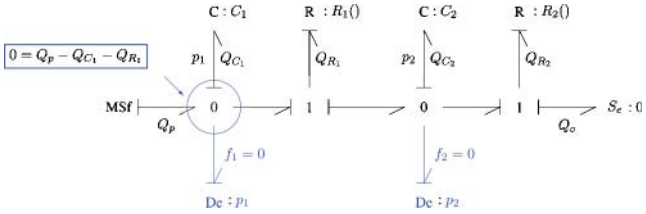

Fig. 2 Bond graph of the hydraulic two-tank system with two pressure sensors

Other sensor placements are also possible. For instance, the volume flow rate through valve 1, Q_{R_1}, and the pressure at the bottom of tank 2 could be monitored. The Df-element in Fig. 3 denotes a flow sensor. This system is also structurally observable. The system is also structurally observable with just one pressure sensor attached to the 0-junction of tank 2, or when the tank pressures and the volume flow rates through both valves are sensed. In the following, the two-tank system with two pressure sensors will be used as an illustrative example.

2.2 Derivation of analytical redundancy relations from a causal bond graph

ARRs will be derived from those bond graph junctions with a detector attached to them.

The left-hand-side encircled 0-junction in the bond graph of Fig. 2 provides the continuity equation for the volume flow rates

$$0 = Q_{\mathrm{p}} - Q_{C_1} - Q_{R_1} \tag{1}$$

If, in this equation, the left-hand-side zero is replaced by a residual, res_1, and if the constitutive equations of the energy C-store, C_1, and of the hydraulic resistor, R_1, are inserted, then equation (1) reads

$$res_1 = Q_{\mathrm{p}} - C_1\dot{p}_1 - k_1 \mathrm{sign}(p_1 - p_2)\sqrt{|p_1 - p_2|} \tag{2}$$

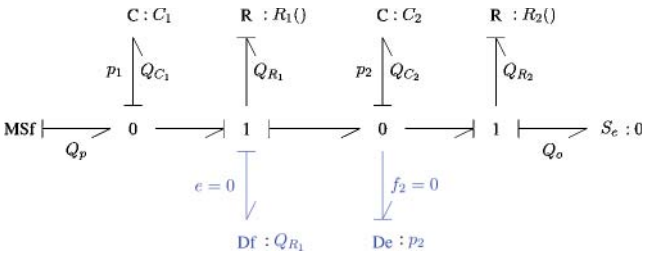

Fig. 3 Bond graph of the hydraulic two-tank system with a flow and a pressure sensor

The right-hand side of this equation only includes known variables and known component parameters, because the pressures in the tanks are measured output variables as indicated by the two effort detectors in Fig. 2. That is, equation (2) is an ARR.

Likewise, the sum of all volume flow rates at the right-side 0-junctions

$$0 = Q_{R_1} - Q_{C_2} - Q_{R_2} \tag{3}$$

leads to an ARR for residual res_2

$$res_2 = k_1 \mathrm{sign}(p_1 - p_2)\sqrt{|p_1 - p_2|} - C_2\dot{p}_2 - k_2\sqrt{p_2} \tag{4}$$

2.3 Structural fault signature matrix

In equation (2), tank 1, T_1, contributes the parameter C_1 and the valve, V_1, between both tanks the parameter k_1. From this view of ARRs, a so-called occurrence matrix can be set up with one row for each known variable or component parameter and one column for each residual. If the occurrence of a variable or a parameter in an ARR is indicated by '1' and its absence by '0', then the result is a binary matrix. It indicates which components contribute to which residual. This matrix is usually augmented by two other columns. The first one with the heading D indicates whether a fault can be detected. The second additional column with the heading I indicates whether a fault can be isolated [**13**], or, in other words, can be identified unequivocally as the cause of a failure among other possible faults in one or several system components. If this is feasible, then it is marked by '1', otherwise by '0'. A fault can be detected if there is at least one non-zero entry in that row. This is indicated by '1' in the first additional column, otherwise by '0'. The augmented matrix is called a *fault signature matrix*. Its columns are called fault signatures (of the ARRs of the residuals). Its rows display the fault signatures of components. Table 1 shows the fault signature matrix of the hydraulic two-tank system with two pressure sensors.

The fault signature matrix of the two-tank system with two pressure sensors includes only two residuals although each 1-junction in the bond graph also contributes a continuity equation for the efforts. These equations could be transformed into ARRs. However, their signatures turn out to be identical to those already listed in the fault signature matrix. Thus, there are only two *structurally* independent residuals in the bond graph model of the two-tank system. In fact, consider, for instance, the sum of efforts at the 1-junction representing the volume

Table 1 Structural fault signature matrix of the two-tank system with two pressure sensors

Component	Variable/parameter	res_1	res_2	D	I
Pump	Q_p	1	0	1	0
Pressure sensor 1	p_1	1	1	1	0
Pressure sensor 2	p_2	1	1	1	0
Tank 1	$C_1 = A_{T_1}/(\rho g)$	1	0	1	0
Tank 2	$C_2 = A_{T_2}/(\rho g)$	0	1	1	0
Valve 1	$k_1 = c_d A_{V_1}\sqrt{2/\rho}$	1	1	1	0
Valve 2	$k_2 = c_d A_{V_2}\sqrt{2/\rho}$	0	1	1	0

flow rate, Q_{R_1}, through valve 1 between the two tanks. If the pressure drop across valve 1 is expressed by the known volume flow rate of the pump, Q_p, and the measured pressure in the first tank, T_1, then the residual, res_3, of the continuity equation of this 1-junction reads

$$0 = p_1 - p_2 - \frac{1}{k_1^2}\ Q_p - C_1\dot{p}_1\ ^2 \text{sign}\ Q_p - C_1\dot{p}_1 = res_3 \tag{5}$$

Clearly, the signature of res_3 is structurally identical to the one of res_1.

2.4 Fault isolation

The fault signature matrix of the two-tank system with two pressure sensors shows that all faults can be detected, but none of them can be isolated. In fact, if, for a given time instant, t, for instance, only residual res_2 is above a given threshold, the reason may be either a leakage from the second tank or a fault in its outlet valve V_2. Clearly, a single fault can be located (isolated), if it can be detected and if the pattern of non-zero entries in the corresponding row of the matrix is unique.

Adding a flow sensor (Df) that measures the volume flow rate through valve 2 allows an observer to distinguish between a leakage from tank 2 and a fault in valve 2. In this case, the constitutive equation of valve 2 provides the ARR

$$res_4 = Q_o - k_2\sqrt{p_2} \neq 0 \tag{6}$$

and the structural fault signature matrix takes the form given in Table 2. In the fault signature matrix of Table 2, the fault signatures of tank 2 and valve 2 are unique. Consequently, faults in these two components can be isolated. If it is assumed that sensors are not faulty, then their rows can be eliminated from the fault signature matrix.

For the two-tank system with two pressure sensors, the number of structurally independent residuals is two. In the second case with two pressure sensors and a flow sensor, their number is three. In general, for an observable system, their number is equal to the number of sensors present in the system [**7**].

Finally, note that for obtaining a structural fault signature matrix it is not necessary to establish model equations and to eliminate unknown variables. A structural fault signature matrix can be set up directly by inspection of causal paths in a causal bond graph [**17**, **18**] regardless of the special form of non-linear constitutive element equations. It is sufficient to know which of the two conjugate variables at a power port has been assigned the role of an input variable. In the previous two subsections, ARRs for the illustrative two-tank example have been determined analytically for pedagogical reasons and for convenience.

3 RESIDUAL BOND GRAPH SINKS

This section explains and motivates residual bond graph sinks. These elements have been used for different purposes, but, to the author's knowledge, they have not been used in bond graph model-based quantitative FDI so far.

Table 2 Structural fault signature matrix of the two-tank system with two pressure sensors and a flow sensor

Component	Variable/parameter	res_1	res_2	res_4	D	I
Pump	Q_p	1	0	0	1	0
Pressure sensor 1	p_1	1	1	0	1	0
Pressure sensor 2	p_2	1	1	1	1	1
Flow sensor	Q_0	0	0	1	1	1
Tank 1	$C_1 = A_{T_1}/(\rho g)$	1	0	0	1	0
Tank 2	$C_2 = A_{T_2}/(\rho g)$	0	1	0	1	1
Valve 1	$k_1 = c_d A_{V_1}\sqrt{2/\rho}$	1	1	0	1	0
Valve 2	$k_2 = c_d A_{V_2}\sqrt{2/\rho}$	0	1	1	1	1

A *residual* bond graph sink is a bond graph sink that adjusts its output power variable so that the power conjugated variable into the sink vanishes. Figure 4 shows a graphical representation according to Bos [**29**]. It explicitly depicts the internal modulation of the sink. In this case, the difference of efforts, $\Delta e := e_1 - \tilde{e}_1$, into the modulated flow sink is sensed. It controls the output of the sink, f, such that the difference, Δe, is driven to zero. The difference Δe can be considered the residual of the 1-junction. If there is no such difference, the output, f, of the residual sink is zero. The latter is equal to the residual, *res*, of the upper 0-junction. For brevity, we will denote residual sinks by *rSf* or *rSe*, respectively. They can be used for different purposes, e.g. for representing internal constraint forces or moments in bodies [**3**, **29**, **30**], i.e. Lagrange multipliers, or for indicating tearing variables in bond graph models [**25**, **26**]. In Karnopp's all-derivative causalities approach to the derivation of Lagrange equations, residual flow sources indicate generalized coordinates. In that context they are know as artificial flow sources [**31**]. Furthermore, in [**32**], Gawthrop and Smith used residual sources for a modification of the standard sequential causality assignment procedure in the case of bond graphs with algebraic loops.

A residual sink results if the parameter of an energy store is assumed to tend to zero. A linear inertia in integral causality with inertance I, for instance, provides a flow such that

$$I \times \dot{f} = \Delta e \tag{7}$$

For $I \to 0$, the constitutive equation of the I energy store turns into the algebraic equation $0 = \Delta e$ or, if zero is replaced by the residual *res*, into the equation

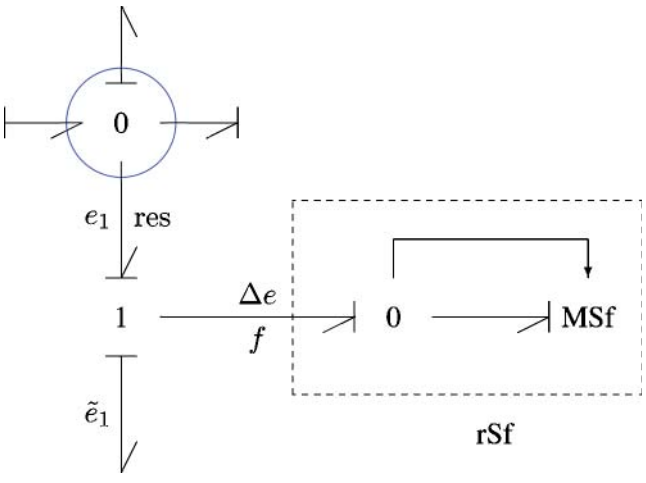

Fig. 4 Representation of a residual flow sink according to Bos [**29**]

$res = \Delta e$. Now, the flow is no longer the output variable of an I energy store in integral causality. It is not a state variable anymore. It is rather a variable determined by the algebraic equation $0 = \Delta e$. As the derivative of f has vanished, while f itself is still an unknown, the mathematical model now is a DAE system and the flow, f, can be considered a component of a descriptor vector. As causal bond graphs express relations between power variables and do not explicitly account for relations between generalized displacements, DAE systems derived from bond graphs are, in general, of index $\leqslant 2$.

In the following, it is shown that these residual bond graph sinks can also be used for numerical computation of fault indicators.

4 COUPLING THE MODELS OF REAL AND FAULTLESS PROCESS BY RESIDUAL SINKS

Model-based FDI starts from the comparison of the actual behaviour of a process engineering system with that of the ideal, faultless system. Signals from the real engineering process can be obtained by means of sensors and can be fed into the model of the faultless process. However, the deliberate introduction of faults into a real engineering process for test purposes may lead to hazardous situations, even to periods of process instability if the equipment allows for introduction of faults at all. Therefore, it is obvious to replace the real process by a behavioural model which enables the introduction of all kinds of faults without risk, and to analyse various fault scenarios through simulation. In an *offline* simulation, residuals of ARRs, being indicators for faults, are numerically evaluated along with the simultaneous solution of the equations of real and faultless process models. This approach [**15**] has the advantage that there is no need for elimination of unknown variables from continuity equations in order to obtain ARRs in *symbolic* form, because a set of coupled equations determining residuals is solved *numerically*. In general, non-linear constitutive equations of elements may even prevent the generation of ARRs in symbolic form.

In contrast to the method in reference [**15**], this paper proposes to couple the real engineering process model to a model of the faultless process by means of residual bond graph sinks introduced in the previous section and to use *integral* causality as the *preferred* computational causality in both bond graph models so that there is no need for numerical differentiation. Signals from the behavioural real

process model, sensed by detectors De or Df respectively, control modulated sources. Their output values are compared with corresponding values from the model of the faultless process.

The real engineering process model accounts for faults by means of modulated sources that can be switched on and off (modelling leakage from the tanks) and by modulated resistors with a time-dependent parameter (modelling partial blockage of the valves). These elements allow for analysing various fault scenarios by deliberately introducing one single fault at a time. If no faults are introduced into the real process model, then the difference between 'measured' signals and their corresponding signals from the faultless process model, theoretically, is equal to zero. The difference is input into the residual sinks. If it vanishes, the output of a residual sink is equal to zero. However, if a process variable differs from the corresponding variable in the faultless process model owing to a fault introduced into the real process model, the residual sink provides a flow or an effort, respectively in order to adapt the faultless process model's behaviour to the perturbed process behaviour and to force the difference to zero (cf. Fig. 5). This non-zero output of a residual sink is equal to a residual of an ARR and is a numerical indicator to a fault.

Introducing various single faults in the real process model, one at a time, and performing simulation runs on the basis of the two coupled process models, are a fast mean to test which residuals are sensitive to which faults.

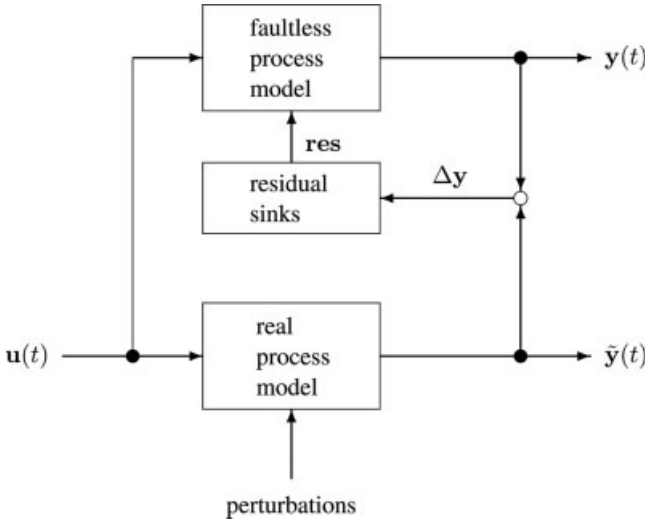

Fig. 5 Coupling the models of real and faultless process by residual sinks

5 APPLICATION EXAMPLE

For illustration, the proposed simulation supported bond graph approach to quantitative fault detection based on the use of residual sinks is applied to a hydraulic two-tank system as a simple example of a process engineering system. For simplicity, only the mass flow is considered, not the associated thermal convection. First, the non-controlled system depicted in Fig. 1 is considered.

5.1 The non-controlled system

In Fig. 6, the lower part of the overall bond graph represents the real process model accounting for faults. A process fault such as leakage from one of the tanks means that an opening in the bottom of the tank reduces the area of the bottom for some period of time. Consequently, the capacity parameter $C_i = A_{T_i}/(\rho g)$ changes abruptly or progressively. Alternatively, leakage from a tank can be modelled by adding a valve to the tank or by means of a modulated flow source as is done in some publications on bond graph model-based FDI (cf. for instance [**16**]). The latter representation is adopted in this paper. A partial blockage of valve V_i is related to a reduction of the valve's parameter k_i (cf. Table 1). Consequently, k_i is a function of time that takes into account the way in which the valve blocks, for instance, abruptly or progressively. In the model of the faulty process the valves are modelled by two modulated resistors. It is assumed that the pressures in the two tanks are 'measured'. Accordingly, effort detectors have been attached to their 0-junctions. The upper part of the overall bond graph represents the faultless process model. Both bond graphs, coupled by means of residual sinks, are submodels of the overall model. The submodel of the real process differs from the faultless process model by the elements that allow for user-introduced faults.

5.1.1 The underlying mathematical model

The integrated model in Fig. 6 has been computed numerically by means of the open-source mathematics package Scilab [**27**]. Formulation of the underlying DAE system in Scilab's mathematical input language is straightforward. The equations can be directly derived from the bond graph of Fig. 6. For the example under consideration, this has been done manually, but could be automated. The Scilab function of the DAE system of the integrated model is displayed in Fig. 7. As required for the formulation of

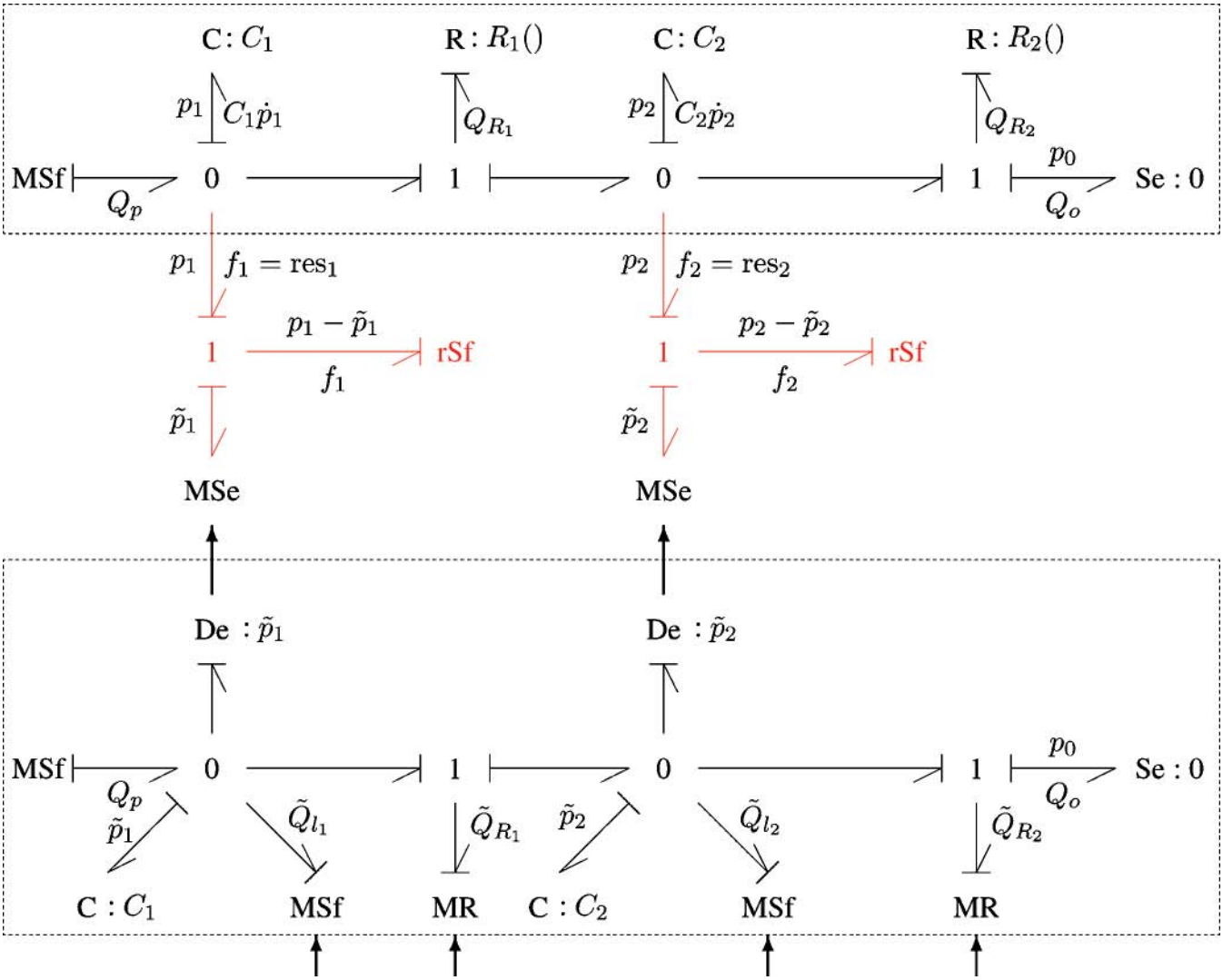

Fig. 6 Coupling of the process model subject to faults (lower part) and the faultless process model (upper part) by means of residual bond graph sinks

DAEs in Scilab input language, the constitutive equations of the energy stores and the equations of the residual sinks have been written in implicit form. The residuals $r(i)$, $i = 1, \ldots, 6$, in the Scilab script are not to be confused with the residuals of the ARRs to be computed. The latter are f_1, f_2. Names of perturbed power variables in the real engineering process model start with the letter t meaning tilde (cf. Fig. 6).

Let $\boldsymbol{x} := [p_1, p_2, \tilde{p}_1, \tilde{p}_2]^{\mathrm{T}}$ be the vector of the state variables and $\boldsymbol{w} := [f_1, f_2]$ the vector of the residuals. Then the DAE system is of the form

$$\dot{\boldsymbol{x}} = \boldsymbol{f}_1(\boldsymbol{x}, \boldsymbol{w}) \tag{8a}$$

$$\boldsymbol{0} = \boldsymbol{f}_2(\boldsymbol{x}, \boldsymbol{w}) \tag{8b}$$

Furthermore, according to the equations in Fig. 7

$$\frac{\partial \boldsymbol{f}_2}{\partial \boldsymbol{x}} = \begin{matrix} 1 & 0 & -1 & 0 \\ 0 & 1 & 0 & -1 \end{matrix} \tag{9}$$

and

$$\frac{\partial \boldsymbol{f}_1}{\partial \boldsymbol{w}} = \begin{bmatrix} -1/C_1 & 0 \\ 0 & -1/C_2 \\ 0 & 0 \\ 0 & 0 \end{bmatrix} \tag{10}$$

Consequently

$$\det \frac{\partial \boldsymbol{f}_2}{\partial \boldsymbol{x}} \frac{\partial \boldsymbol{f}_1}{\partial \boldsymbol{w}} = \det \begin{bmatrix} -1/C_1 & 0 \\ 0 & -1/C_2 \end{bmatrix} = \frac{1}{C_1 C_2} \neq 0 \tag{11}$$

```
// Scilab function with the DAE system of the two tank models
// coupled by residual bond graph sinks
function [r,ires] = daesys(t,x,xdot)

// tank pressures of the faultless process model:
p1   = x(1)
p2   = x(2)
// tank pressures of the process model subject to faults:
tp1  = x(3)
tp2  = x(4)
// residuals:
f1   = x(5)
f2   = x(6)

// xdot: rate of change of the descriptor vector x:
dp1  = xdot(1)
dp2  = xdot(2)
dtp1 = xdot(3)
dtp2 = xdot(4)
//------------
df1  = xdot(5)
df2  = xdot(6)

// system inputs:
Qp   = Flow*pulse(t,tstart,tstop)

// no leakage from the two tanks of the real process model:
tQl1 = 0.0
tQl2 = 0.0

// orifices:
QR1  = orifice(AV1,p1,p2)
QR2  = orifice(AV2,p2,p0)

// partial blockage of valve 1 for 50.0s <= t <= 60.0s:
tQR1 = (1.0 - pulse2(t,50.0,60.0,0.8))*orifice(AV1,tp1,tp2)
tQR2 = orifice(AV2,tp2,p0)

// energy stores:
r(1) = Qp - QR1 - C1*dp1 - f1                  // p1
r(2) = QR1 - QR2 - C2*dp2 - f2                 // p2
r(3) = Qp - tQR1 - tQl1 - C1*dtp1              // tp1
r(4) = tQR1 - tQR2 - tQl2 - C2*dtp2            // tp2

// equations of the residual bond graph sinks:
r(5) = p1 - tp1                                // f1
r(6) = p2 - tp2                                // f2

ires = 0 // successful computation of r
endfunction
```

Fig. 7 Scilab function with the DAE system of the two-tank models coupled by residual sinks

That is, the differential algebraic index of the DAE system is two.

5.1.2 *Simulation of fault scenarios*

For the numerical solution of DAE systems, Scilab provides the widely used DASSL code [**33**]. Solving a DAE system requires a consistent set initial conditions for the components of the descriptor vector and their time derivatives. For the consistent initialization of a DAE system, the algorithm of Pantelides [**34**] can be used. In order to facilitate the specification of a consistent set of initial conditions, it is assumed that the two tanks are empty at initial time $t = 0$ and that the pump delivers a constant volume flow rate, Q_p, for the time period $10.0\,\text{s} \leqslant t \leqslant 40.0\,\text{s}$. That is, the empty tanks are filled for 30 s and then they discharge at a rate depending on how much the valves are open. Figure 8 depicts the undisturbed dynamic behaviour.

Leakage from tank 1. As to this example, two types of potential faults can be considered, namely, leakage from the tanks and partial blockage of the valves. As a first fault scenario, a constant leakage flow from tank 1 is assumed to be effective for the time period $50\,\text{s} \leqslant t \leqslant 60\,\text{s}$, while the two tanks discharge. As a result, the pressures in the tanks decrease at a higher rate during this time period. Figure 9 shows the time evolution of the tank pressures in the case of a leakage from tank 1. Leakage from tank 1 corresponds to a decrease of the area of its bottom. According to the fault signature matrix of Table 1, residual res_1 is affected, while residual res_2 is not. Figures 10 and 11 depicting the residuals f_1 and f_2 validate this expectation. Note that at $t = 60\,\text{s}$ the leakage from tank 1 stops abruptly. The system abruptly returns to normal operation. Accordingly, residual f_1 abruptly drops to zero.

Partial blockage of valve 1. Another fault that may occur is a partial blockage of the valve between the two tanks. If it happens after the pump has switched

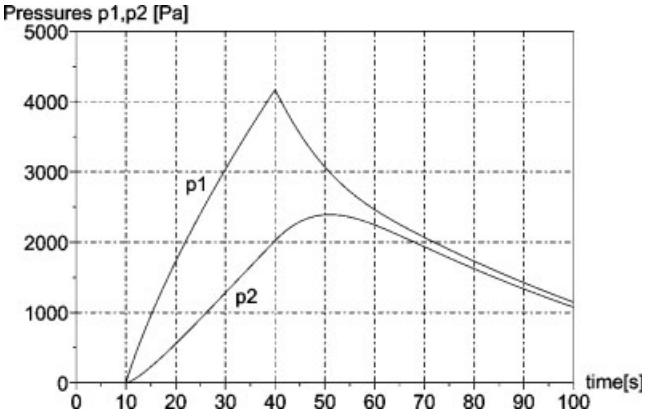

Fig. 8 Tank pressures in the case of no faults

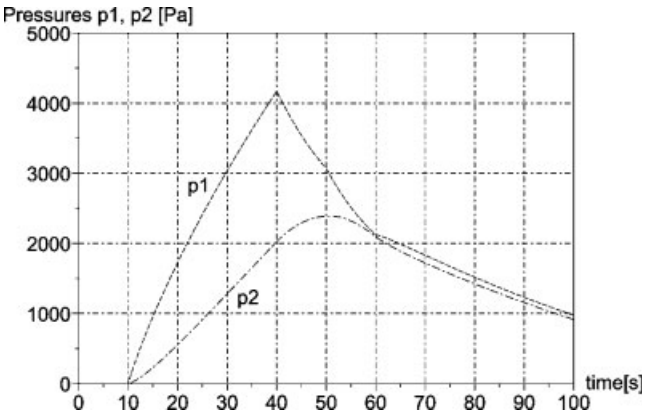

Fig. 9 Tank pressures in the case of a leakage from tank 1

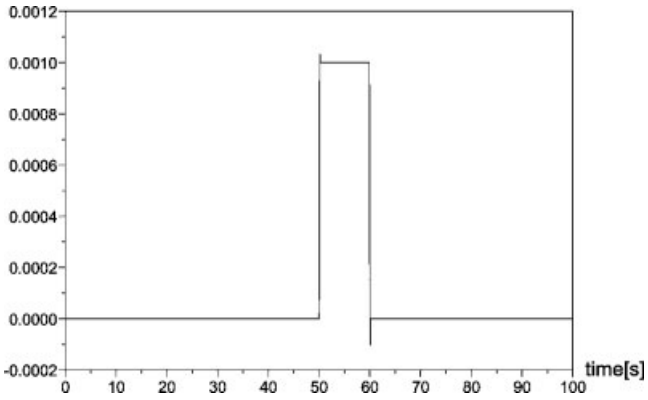

Fig. 10 Residual f_1 in the case of a leakage from tank 1

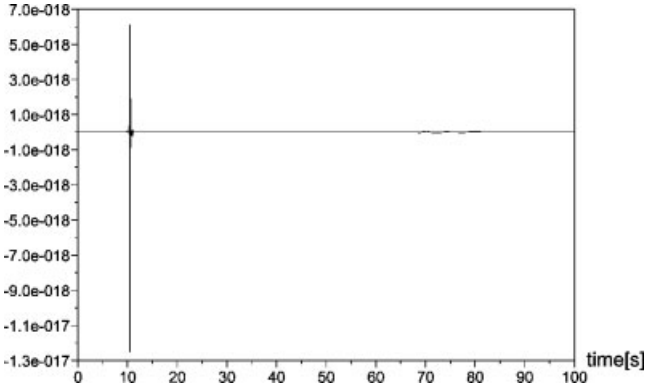

Fig. 11 Residual f_2 in the case of a leakage from tank 1

off, then, during the time period this fault is effective, the pressure in the first tank decreases at a lower rate, while the pressure in the second tank decreases at a higher rate. This can be seen from Fig. 12. According to the fault signature matrix, both residuals are sensitive to a fault in valve 1 connecting both tanks. This is verified by Fig. 13.

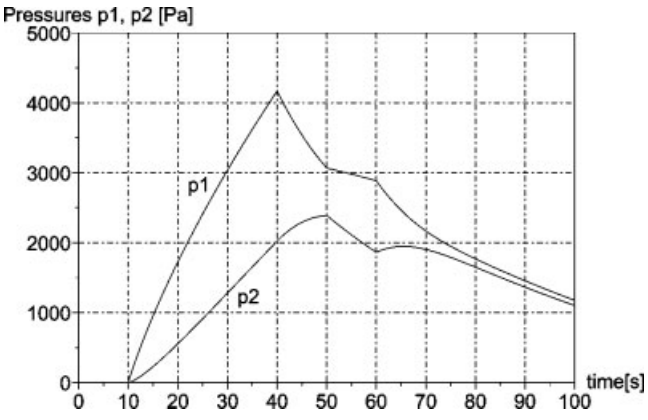

Fig. 12 Tank pressures in the case of a partial blockage of the valve between the two tanks

5.2 The controlled system

With regard to safety, it is important that the closed-loop control of a system is robust in the presence of faults. This is evident, for instance, for the control of the pressure in a covered tank. A precondition for FTC is the detection and isolation of faults in a controlled system. In the following, it is shown that the proposed coupling of a faultless process model to the real process model by means of residual bond graph sinks is also applicable to controlled systems or processes.

For illustration, the fluid level in the second tank of the example system is sensed and is input into a PI controller which controls the feed pump. Accordingly, the constant flow pump is replaced by a flow pump with the characteristic displayed in Fig. 14, where u_p denotes the input signal from the controller and Q_{max} the maximum outflow.

The bond graph of the controlled system is depicted in Fig. 15. Again, the model of the controlled process in Fig. 15 is coupled to a model of the controlled faulty process by means of residual bond graph sinks as displayed in Fig. 16. For numerical computation of the overall model in Fig. 16, again, it is assumed that both tanks are empty at initial time $t = 0$. They are filled by the flow pump until a fluid

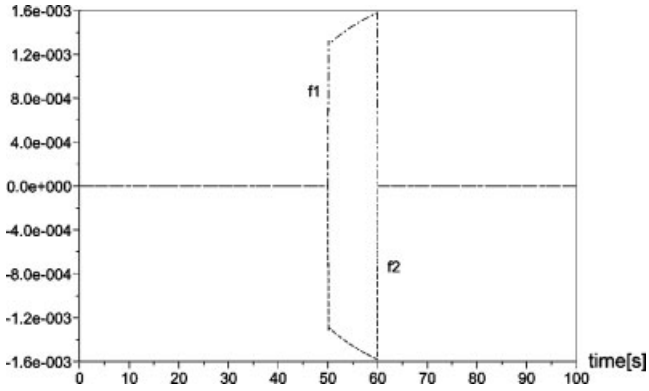

Fig. 13 Residuals f_1 and f_2 due to a partial blockage of the valve between the two tanks

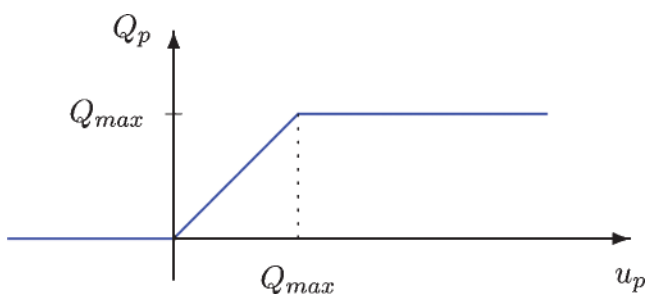

Fig. 14 Characteristic of the controlled flow pump

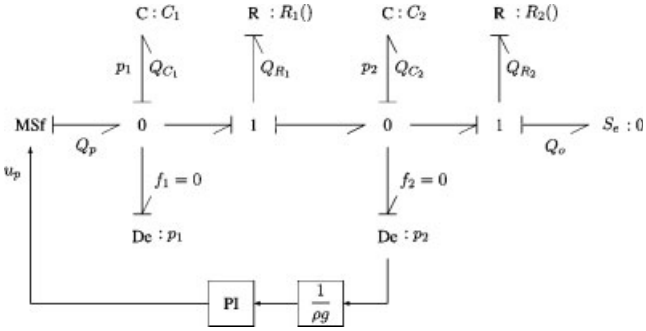

Fig. 15 Bond graph of the controlled two-tank system with two pressure sensors

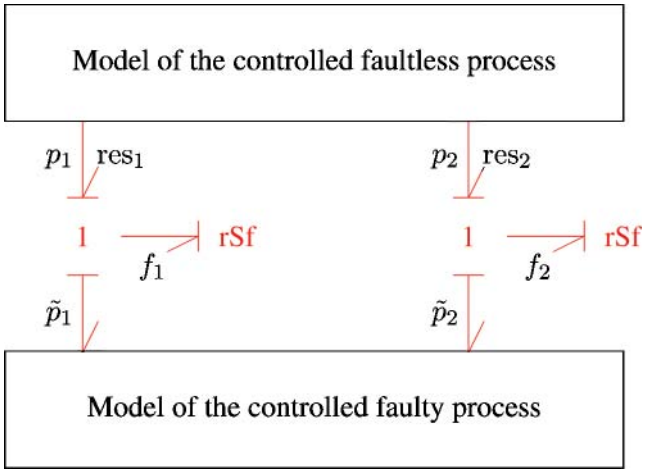

Fig. 16 Coupling of both bond graph models of the controlled process

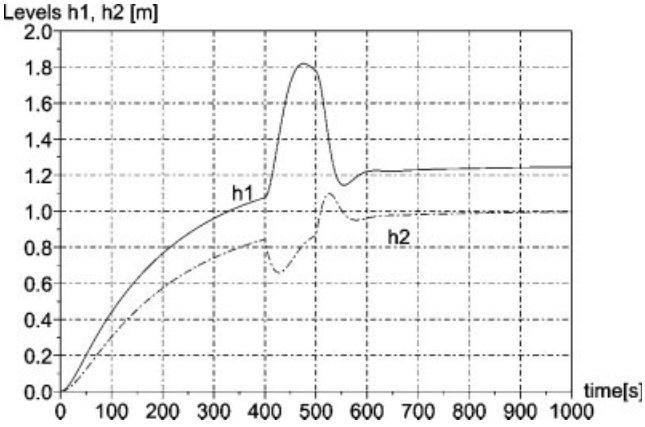

Fig. 17 Fluid levels in both tanks in the case of a leakage from tank 2

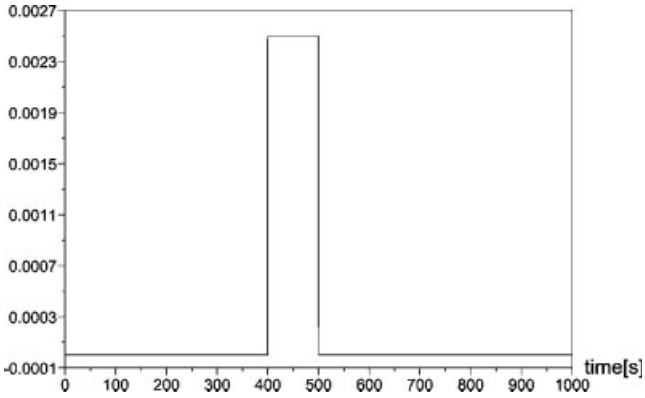

Fig. 18 Residual f_2 in the case of a leakage from tank 2

level of 1 m in the second tank has been reached, while at the same time, there is an outflow Q_o from tank 2. The fluid level in tank 2 is maintained by the PI controller. Its set point is 1 m.

5.2.1 Simulation of a fault scenario

The fault scenario under study is an abruptly occurring leakage from tank 2 lasting for the time period $400\,\text{s} \leqslant t \leqslant 500\,\text{s}$. Figure 17 shows the time history of the fluid levels in both tanks. As can be seen from Fig. 17, the abrupt leakage from tank 2 decreases the fluid level. As a result, the PI controller causes the pump to feed more fluid into tank 1. This leads to a higher fluid level in tank 1, which is decreased by the outflow into tank 2. When the leakage abruptly stops at $t = 500\,\text{s}$, the PI controller ensures that the prescribed fluid level is reached and maintained. Figure 18 shows that an abnormal operation induced by leakage from tank 2 is clearly reflected by the numerically computed time history of residual f_2. In accordance with the fault signature matrix of Table 1, residual f_2 is sensitive to this fault, while f_1 is not.

6 SENSITIVITY OF RESIDUALS

As has been shown in the previous sections, faults in a system are clearly reflected by the numerically computed outputs of residual sinks. If each residual is sensitive to only one fault, faults can unambiguously be identified.

6.1 Residual thresholds

The residual sinks introduced in section 3 react as soon as the difference between a 'measured' signal from a behavioural model of the faulty real engineering process and its corresponding signal from the faultless process model is different from zero. This difference, however, will never be identical to zero over some time span owing to inaccuracies of the numerical computation. Moreover, if measured

signals are provided by real sensors the difference of signals into a residual sink will be affected by sensor noise and uncertainties in the parameters of the engineering process. As a result, a residual sink will produce a non-zero residual that does not necessarily indicate a fault. In order to avoid incorrect fault detection and false alarms in a process supervision system a difference between a measured signal and its corresponding signal from the faultless process model must be allowed to vary within given bounds. The introduced residual sinks can account for a threshold by a small modification. Consider the residual flow sink in Fig. 19. As long as the absolute value of the difference between a measured effort, $\tilde{e}$, and its corresponding effort, e, from the faultless process model, $|\Delta e| := |e - \tilde{e}|$, is below a given threshold, ε, the signal, s, modulating the residual sink is set to zero and the residual sink remains inactive. Otherwise, $|\Delta e|$ is the modulating signal and causes the residual sink to drive the difference to zero

$$s = T(|\Delta e|) = \begin{array}{lll} 0 & \text{if} & |\Delta e| < \varepsilon \\ \Delta e & \text{if} & |\Delta e| \geqslant \varepsilon \end{array} \tag{12}$$

6.2 Sensitivity of residuals to parameter uncertainties

Given numerically computed values of residuals, a natural question is how sensitive they are to parameter uncertainties and which are the parameter uncertainties that affect a residual under consideration most significantly. Clearly, fault detection and isolation should be robust with regard to parameter uncertainties, e.g. owing to tolerances in the manufacturing process of system components, or to faulty parameter identification. In addition to the structural fault signature matrix considered in section 2.3, a matrix can be set up that accounts for sensitivities of residuals. In reference [**11**], such a matrix is called a *practical* fault signature matrix.

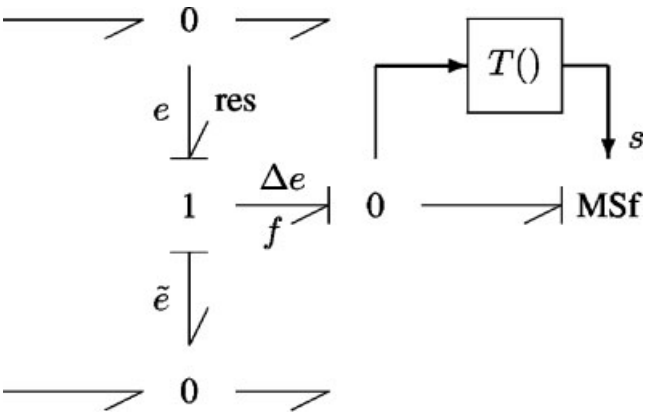

Fig. 19 Residual flow sink with a threshold

In the literature, various bond graph-based approaches to parameter sensitivity analysis have been proposed [**35**–**38**]. Recently, Samamtaray and Ghoshal [**39**] used so-called residual sensitivities to speed up FDI by parameter estimation in the case of *multiple* simultaneously occurring faults. Djeziri *et al.* [**40**] split an ARR into a nominal part and a part due to uncertainties and apply sensitivity analysis to the uncertain part.

In the following, the sensitivity pseudo bond graph approach [**35**, **36**] will be adopted; namely, bonds do not carry power variables e and f respectively, but their partial derivatives with respect to a parameter θ. There can be as many such sensitivity pseudo bond graphs as there are parameters in the model. However, these sensitivity pseudo bond graphs can have the same structure.

6.2.1 *Parameter sensitivity model of a 1-port C energy storage element*

Consider the constitutive equation of a linear 1-port C element with the capacitance C

$$C \times \dot{e}_C = f_C \tag{13}$$

Then, partial differentiation of equation (13) with respect to a parameter θ gives

$$\underbrace{\frac{\partial C}{\partial \theta}}_{=:\, C_\theta} \dot{e}_C + C \underbrace{\frac{\partial \dot{e}_C}{\partial \theta}}_{=:\, \dot{e}_C^s} = \underbrace{\frac{\partial f_C}{\partial \theta}}_{=:\, f_C^s} \tag{14}$$

The factor $c_\theta := \partial C / \partial \theta$ in equation (14) is either equal to one or it vanishes. In any case, equation (14) can be represented by the sensitivity component pseudo bond graph model in Fig. 20 (cf. Borutzky and Granda [**38**]), in which variables, e^s and f^s with a superscript s are taken as 'power' variables. Note that in the sensitivity component pseudo bond graph in Fig. 20 only causal strokes change if the constitutive equation of the C element, equation (13), is written in integral causality form.

6.2.2 *Parameter sensitivity model of a non-linear 1-port orifice*

In the same way, a sensitivity component pseudo bond graph model can be found for a non-linear 1-

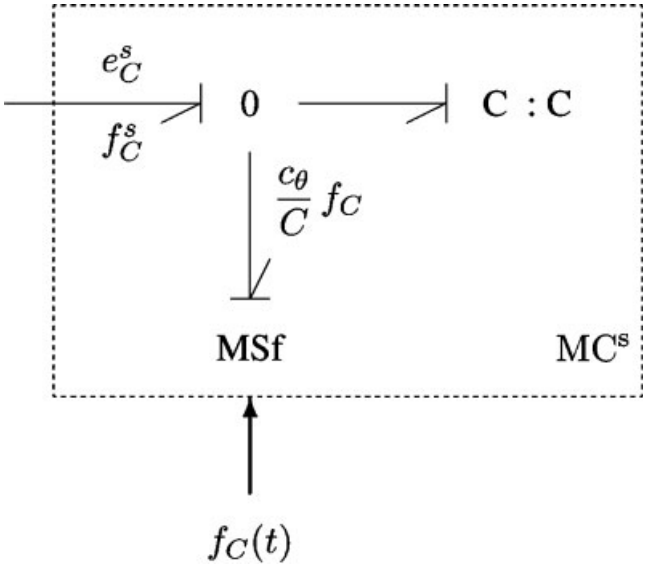

Fig. 20 Sensitivity pseudo bond graph of a linear 1-port C storage element

port orifice. Consider the constitutive equation of an orifice of cross-section area A assuming that the pressure drop across the orifice, Δp, is non-negative

$$Q_R = \underbrace{c_d A\sqrt{2/\rho}}_{=:\,k} \times \sqrt{\Delta p} \tag{15}$$

where c_d denotes the discharge coefficient. Partial differentiation with respect to a parameter θ yields

$$\underbrace{\frac{\partial Q_R}{\partial \theta}}_{=:\,f_R^s} = \underbrace{\frac{\partial k}{\partial \theta}}_{=:\,k_\theta} \sqrt{\Delta p} + k \times \frac{1}{2\sqrt{\Delta p}} \times \underbrace{\frac{\partial \Delta p}{\partial \theta}}_{=:\,e_R^s} \tag{16}$$

equation (16) can be represented by the sensitivity component pseudo bond graph model in Fig. 21. Note that this submodel also holds if the constitutive equation of an orifice is written in resistance causality, that is, $\Delta p = Q_R^2\ k^2$. Only causalities at the submodel's power port and at the MR element change.

6.2.3 *Adding a sensitivity pseudo bond graph to the faultless process model*

With these two sensitivity component pseudo bond graph models, a sensitivity pseudo bond graph (SPBG) of the two-tank system can be constructed. It has the same structure as the bond graph of the system depicted in Fig. 2. Note that this construction of an SPBG as a companion of a given bond graph is

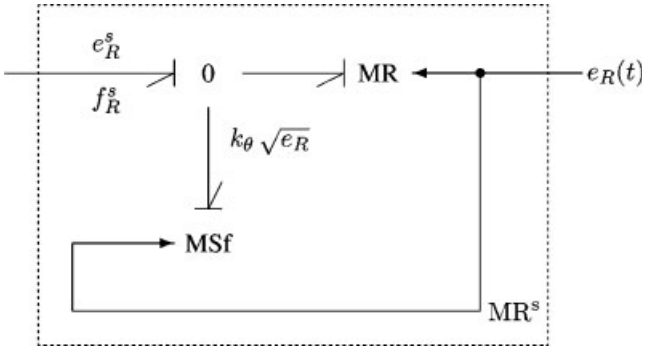

Fig. 21 Sensitivity pseudo bond graph of a non-linear 1-port orifice

not limited to the example under consideration. For all other bond graph elements sensitivity component models can be developed as well. The sensitivity model of a 1-junction (0-junction) again is a 1-junction (0-junction). Clearly, sources providing a signal independent of any element parameter become sources of value zero. The structure of the sensitivity bond graph differs from the one of the initial bond graph only by additional sources (cf. [**38**]).

The SPBG is coupled to the faultless process model of the two-tank system as displayed in Fig. 22. Parameters in the behavioural model of the faulty real engineering process can be stochastic variables with a certain distribution, a mean value, and a standard deviation. Moreover, to make the behavioural real process model even more realistic, noise can be taken into account. In that case, signals provided by detectors must be input into appropriate filters before they are used in the comparison with signals from the faultless process model. Now, sensitivities of residuals can be sensed by flow detectors as shown in the upper part of the integrated bond graph in Fig. 22. In fact, for instance, summing up 'flow' variables at the right-hand-side 0-junction in the SPBG part yields

$$\frac{\partial}{\partial \theta} res_2(t) = f_{R_1}^s(t) - f_{C_2}^s(t) - f_{R_2}^s(t) \tag{17}$$

or

$$\frac{\partial}{\partial \theta} res_2(t) = \frac{\partial Q_{R_1}}{\partial \theta}(t) - \frac{\partial Q_{C_2}}{\partial \theta}(t) - \frac{\partial Q_{R_2}}{\partial \theta}(t) \tag{18}$$

Equation (18) is equivalent to the one obtained by partial differentiation of equation (4) assuming

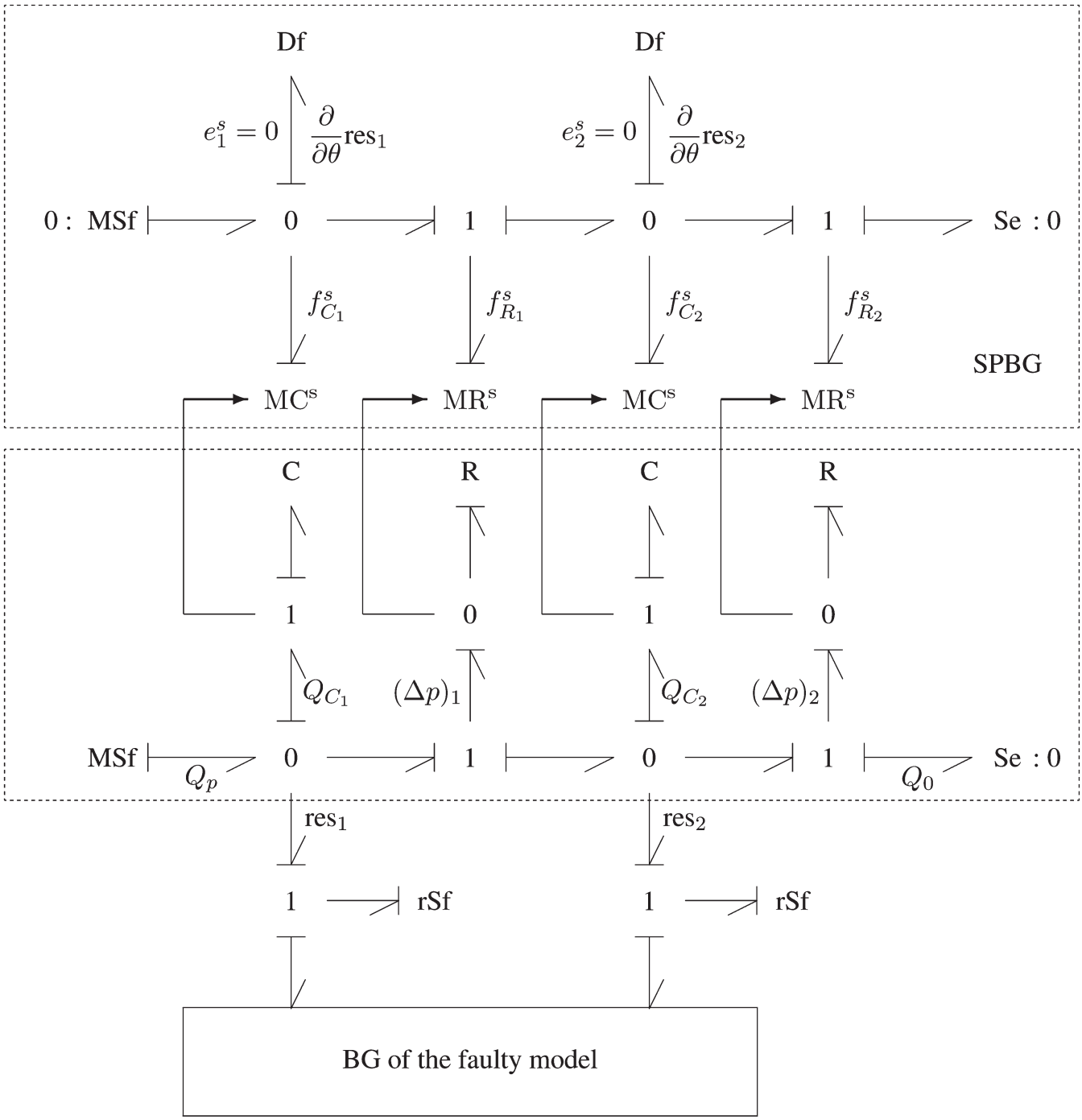

Fig. 22 SPBG (upper part) and bond graph of the two-tank system coupled together

$p_1 \geqslant p_2$. The 'flow' variables on the right-hand side of equation (17) are the outputs of the sensitivity component pseudo bond graph models of the corresponding C and R elements in the bond graph of the two-tank system. The information needed to compute them is provided by these elements as indicated in Fig. 22. That is, residuals and their sensitivities with respect to a parameter can be computed numerically at the same time.

In the SPBG part of Fig. 22 the two flow detectors entail derivative causality at the MC^s elements. These elements are not by default in derivative causality. They can take integral causality as well, as pointed out in section 6.2.1. However, as flow detectors do not impose an effort different from zero while measuring a flow, the input into the MC^s elements in derivative causality is zero. Consequently, no numerical differentiation of an input

different from zero has to be performed and the MC^s submodel (cf. Fig. 20) reduces to a flow sink modulated by a flow computed in the faultless process model. Other sensor placements, e.g. the one depicted in Fig. 3, are also possible, but they also do not entail numerical differentiation of a non-zero input.

7 CONCLUSIONS

A bond graph approach to the *numerical* computation of fault indicators in quantitative model-based fault detection based on the use of residual sinks has been presented. The approach especially aims at models with non-linearities that make it cumbersome or even impossible to derive ARRs from model equations in symbolic form by eliminating unknown variables.

A behavioural model of an engineering process subject to faults is coupled to a faultless process model by means of *residual bond graph sinks*. The approach has the following advantages.

1. The residual bond graph sinks have a clear and intuitive role. They provide an effort or a flow respectively that forces the difference between a monitored variable and its corresponding variable from the faultless process model to zero, and adapts the latter to the signal perturbed by a fault. At the same time, the output of a residual sink is the residual of an ARR.
2. Furthermore, in order to avoid incorrect fault detection, residual sinks can account for given residual thresholds.
3. Unknown variables do not need to be eliminated from model equations in order to obtain ARRs in *symbolic* form. Residuals as fault indicators are computed numerically as components of a descriptor vector of a DAE system.
4. Standard bond graph methodology can be used to construct both a behavioural model of a real engineering process and a faultless process model, and to assign preferred *integral* computational causality in both models. There is no need for numerical differentiation.
5. The DAE system derived from the coupled bond graph models can be solved numerically by means of the widely used DASSL code.
6. By means of offline simulation runs, the impact of all kinds of faults can be studied without risk. In the case of thermodynamic processes, 'signals' from the simulated faulty process can be obtained much faster than from the real process.
7. In addition to residuals, parameter sensitivities of residuals can also be computed numerically at the same time. To that end, a sensitivity pseudo bond graph can be systematically constructed from the faultless process model. It has the same structure as the faultless process model. Apart from junctions, its sensitivity models of bond graph elements are, in general, modulated by power variables from the faultless process model. The placement of sensors detecting parameter sensitivities of residuals may entail that some sensitivity submodels of 1-port energy stores take derivative causality. This, however, does not necessarily mean that numerical differentiation of a variable different from zero has to be performed. Information about sensitivities of residuals can be used for setting up another fault signature matrix that can serve in fault accommodation.

REFERENCES

1 **Isermann, R.** Model-based fault-detection and diagnosis – status and applications. *Ann. Rev. Control*, 2005, **29**, 71–85.
2 **Karnopp, D. C., Margolis, D. L.,** and **Rosenberg, R. C.** *System dynamics – modeling and simulation of mechatronic systems,* fourth edition, 2005 (Wiley).
3 **Borutzky, W.** *Bond graphs – a methodology for modelling multidisciplinary dynamic systems*, 2004 (SCS Publishing House, Erlangen, Germany).
4 **Dauphin-Tanguy, G.** *Les bond graphs*, 2000 (Hermes Science Europe Ltd, Paris, France).
5 **Mukherjee, A.** and **Karmakar, R.** *Modelling and simulation of engineering systems through bond-graphs*, 2000 (Narosa Publishing House, New Delhi, India).
6 **Gawthrop, P.** and **Smith, L.** *Metamodelling: bond graphs and dynamic systems*, 1996 (Prentice Hall, Hemel Hempstead, UK).
7 **Mukherjee, A., Karmakar, R.,** and **Samantaray, A. K.** *Bond graph in modeling, simulation and fault identification*, 2006 (I.K. International Publishing House, New Delhi, India).
8 **Thoma, J.** and **Bouamama, B. O.** *Modeling and simulation in thermal and chemical engineering (a bond graph approach)*, 2000 (Springer-Verlag, Berlin).
9 **Heny, C., Simanca, D.,** and **Delgado, M.** Pseudo-bond graph model and simulation of a continuous stirred tank reactor. *J. Franklin Inst.*, 2000, **337**, 21–42.
10 **Bouamama, B. O., Medjaher, K., Samantaray, A. K.,** and **Staroswiecki, M.** Supervision of an industrial steam generator. Part I: bond graph modelling. *Control Engng Pract.*, 2006, **14**(1), 71–83.

11 **Medjaher, K., Samantaray, A. K., Bouamama, B. O.,** and **Staroswiecki, M.** Supervision of an industrial steam generator. Part II: online implementation. *Control Engng Pract.*, 2006, **14**(1), 85–96.

12 **Feenstra, P. J., Mosterman, P. J., Biswas, G.,** and **Breedveld, P. C.** Bond graph modeling procedures for fault detection and isolation of complex flow processes. In Proceedings of the International Conference on *Bond graph modeling* (Eds J. J. Granda and G. Dauphin-Tanguy), Phoenix, Arizona, USA, 7–11 January 2001, pp. 77–82 (SCS Publishing).

13 **Bouamama, B. O., Samantaray, A. K., Staroswiecki, M.,** and **Dauphin-Tanguy, G.** Derivation of constraint relations from bond graph models for fault detection and isolation. In Proceedings of the International Conference on *Bond graph modeling*, (Eds J. J. Granda and F. Cellier), Orlando, Florida, USA, 19–23 January 2003, pp. 104–109. (SCS Publishing).

14 **Sia, K.** and **Naamane, A.** Bond graph: a suitable tool for component fault diagnosis. In Proceedings of the International Conference on *Bond graph modeling* (Eds J. J. Granda and F. Cellier), Orlando, Florida, USA, 19–23 January 2003, pp. 89–103 (SCS Publishing).

15 **Medjaher, K., Samantaray, A. K.,** and **Bouamama, B. O.** Diagnostic bond graphs for direct residual evaluation. In Proceedings of the International Conference on *Bond graph modeling* (Eds J. J. Granda and F. Cellier), New Orleans, Louisiana, USA, 23–27 January 2005, pp. 307–312 (SCS Publishing).

16 **Ghoshal, S. K., Samantaray, A. K.,** and **Mukherjee, A.** Improvements to single fault isolation using estimated parameters. In Proceedings of the International Conference on *Bond graph modeling* (Eds J. J. Granda and F. Cellier), New Orleans, Louisiana, USA, 23–27 January 2005, pp. 301–306 (SCS Publishing).

17 **Samantaray, A. K., Medjaher, K., Bouamama, B. O., Staroswiecki, M.,** and **Dauphin-Tanguy, G.** Diagnostic bond graphs for online fault detection and isolation. *Simul. Modelling Pract. Theory*, 2006, **14**(3), 237–262.

18 **Borutzky, W.** Residual bond graph sinks for numerical evaluation of analytical redundancy relations in model based single fault detection and isolation. In Proceedings of the 20th European Conference on *Modelling and simulation*, Sankt Augustin, Germany, 28–31 May 2006, pp. 166–172.

19 **Ghoshal, S. K.** Model-based fault diagnosis and accommodation using analytical redundancy: a bond graph approach. Department of Mechanical Engineering, Indian Institute of Technology, Kharagpur, India 2006.

20 **Gertler, J.** *Fault detection and diagnosis in engineering systems*, 1998 (Marcel Dekker, New York).

21 **Blanke, M., Kinnaert, M., Lunze, J.,** and **Staroswiecki, M.** *Diagnosis and fault-tolerant control*, 2003 (Springer Verlag, Berlin).

22 **Ding, S.** *Model-based fault diagnosis techniques*, 2008 (Springer Verlag, Berlin).

23 **Tagina, M., Cassar, J. P., Dauphin-Tanguy, G.,** and **Staroswiecki, M.** Monitoring of systems modelled by bond-graphs. In Proceedings of the International Conference on *Bond graph modeling and simulation* (Eds J. J. Granda and F. Cellier), Las Vegas, USA, 15–18 January 1995, pp. 275–280 (SCS Publishing).

24 **Staroswiecki, M.** and **Comtet-Varga, G.** Analytical redundancy relations for fault detection and isolation in algebraic dynamic systems. *Automatica*, 2001, **37**, 687–699.

25 **Borutzky, W.** and **Cellier, F. E.** Tearing algebraic loops in bond graphs. *Trans. SCS*, 1996, **13**(2), 102–115.

26 **Borutzky, W.** Supporting the generation of a state space model by adding tearing information to the bond graph. *Simul. Pract. Theory*, 1999, **7**(5/6), 419–438.

27 **Scilab Consortium.** Scilab, available from: http://www.scilab.org (accessed Nov. 2008).

28 **Dauphin-Tanguy, G., Rahmani, A.,** and **Sueur, C.** Bond graph aided design of controlled systems. *Simul. Pract. Theory*, 1979, **7**(5/6), 493–513.

29 **Bos, A. M.** Modelling multibody systems in terms of multibond graphs with application to a motorcycle. University of Twente, Enschede, The Netherlands, 1986.

30 **Félez, J., Vera, C., José, I. S.,** and **Cacho, R.** BONDYN: a bond graph based simulation program for multibody systems. *Trans. ASME, J. Dyn. Sys., Measmt. Control*, 1990, **112**, 717–727.

31 **Karnopp, D.** Lagrange's equations for complex bond graph systems. *Trans. ASME, J. Dyn. Sys., Measmt. Control*, 1977, **99**(4), 300–306.

32 **Gawthrop, P.** and **Smith, L.** Causal augmentation of bond graphs with algebraic loops. *J. Franklin Inst.*, 1992, **329**, 291–303.

33 **Brenan, K. E., Campbell, S. L.,** and **Petzold, L. R.** *Numerical solution of initial-value problems in differential-algebraic equations*, 1996 (SIAM, Philadelphia, PA).

34 **Pantelides, C. C.** The consistent initialization of differential-algebraic systems. *SIAM J. Sci. Stat. Comput.*, 1988, **9**, 213–231.

35 **Cabanellas, J. M., Félez, J.,** and **Vera, C.** A formulation of the sensitivity analysis for dynamic systems optimization based on pseudo bond graphs. In Proceedings of the International Conference on *Bond graph modeling and simulation*, 1995, pp. 135–144 (SCS Publishing).

36 **Gawthrop, P.** Sensitivity bond graphs. *J. Franklin Inst.*, 2000, **337**, 907–922.

37 **Kam, C. S.** and **Dauphin-Tanguy, G.** Sensitivity function determination on a bond graph model. In Proceedings of the 13th European Simulation Symposium: *Simulation in industry*, Marseille, France, 18–20 October 2001, pp. 735–739 (SCS Publishing).

38 **Borutzky, W.** and **Granda, J.** Bond graph based frequency domain sensitivity analysis of multi-disciplinary systems. *Proc. Instn Mech. Engrs, Part I: J. Systems and Control Engineering*, 2002, **216**(I1), 85–99.
39 **Samantaray, A. K.** and **Ghoshal, S. K.** Sensitivity bond graph approach to multiple fault isolation through parameter estimation. *Proc. IMechE, Part I: J. Systems and Control Engineering*, 2007, **221**(I4), 577–587.
40 **Djeziri, M. A., Merzouki, R., Bouamama, B. O.,** and **Dauphin-Tanguy, G.** Bond graph model based for robust fault diagnosis. In Proceedings of the 2007 American Control Conference, New York City, USA, 11–13 July 2007, pp. 3017–3022 (IEEE, Piscataway, NJ).

APPENDIX 1

Notation

A_T	cross-sectional area of a tank
A_V	cross-sectional area of a valve orifice
c_d	discharge coefficient of a valve orifice
e	effort variable at a power port of an element or component
e^s	'effort' variable in the corresponding SPBG of a bond graph
f	flow variable at a power port of an element or component
f^s	'flow' variable in the corresponding SPBG of a bond graph
g	gravitational acceleration ($9.81\,\mathrm{m/s^2}$)
MR	R element with a signal modulated resistance
MC^s	SPBG of a linear 1-port C storage element
MC^s	SPBG of a non-linear 1-port orifice
p	tank pressure
Q	volume flow rate
res	residual of an ARR
t	time
T	tank
$u(t)$	system input
V	valve
$y(t)$	system output
$\tilde{y}(t)$	perturbed system output
θ	model parameter
ρ	fluid density (assumed constant)

APPENDIX 2

```
// Parameters of the non-controlled hydraulic two tank example
//
// Gravitational acceleration:
g = 9.81; // [m/s^2]
// Oil density:
rho = 780.0; // [kg/m^3]
// Discharge coefficient:
c_d = 0.61;
r = c_d*sqrt(2/rho);
//
// Cross-sectional area of the tanks:
AT1 = 1.53e - 1; // [m^2]
AT2 = AT1;
// Capacitances of tanks:
C1 = AT1/(rho*g);
C2 = C1;
// Cross-sectional area of the valves:
AV1 = 0.2e - 2; // [m^2]
AV2 = 0.1e - 2; // [m^2]
//
// Flow of the pump:
Flow = 0.5e - 2; // [m^3/s]
//
// Leakage from tank T_1:
Ql = 0.1e - 2; // [m^3/s]
//
// Pressure of the environment:
p0 = 0.0; // [Pa]
//
// Initial conditions:
//
// Tanks are empty at t = t0;
// no flows into and out of the tanks at t = t0:
y0 = [0.0;0.0;0.0;0.0;0.0;0.0];
ydot0 = [0.0;0.0;0.0;0.0;0.0;0.0];
//
// Parameters of the controlled two-tank system
//
// Parameters of the PI controller:
Kp = 2.0e - 2; // proportional gain
Ki = 1.0e - 4; // integral gain
SP = 1.0; // [m], set point
//
// Pump:
// maximum outflow
Qmax = 1.0e - 2; // [m^3/s]
```